



ELSEVIER

Available online at www.sciencedirect.com

SCIENCE @ DIRECT®

Journal of Constructional Steel Research 61 (2005) 1435–1446

JOURNAL OF
CONSTRUCTIONAL
STEEL RESEARCH

www.elsevier.com/locate/jcsr

Experimental and numerical research on the critical temperature of laterally unrestrained steel I beams

L.M.R. Mesquita^a, P.A.G. Piloto^{a,*}, M.A.P. Vaz^b,
P.M.M. Vila Real^c

^a*Applied Mechanics Department, Polytechnic Institute of Bragança, Ap. 1134, 5301-857 Bragança, Portugal*

^b*Mechanical Department, Faculty of Engineering of University of Porto, Rua Dr. Roberto Frias, 4200-465 Porto, Portugal*

^c*Civil Department, University of Aveiro, Campus Santiago, 3810-193 Aveiro, Portugal*

Received 20 September 2004; accepted 29 April 2005

Abstract

Lateral unrestrained steel beams when subjected to high temperatures may collapse in service by lateral torsional buckling. This instability state may be predicted in the resistance, temperature and time domain. In this work the beam strength is determined in the temperature domain from a batch of numerical and experimental tests, with a specified degree of utilisation and a typical accident temperature rise.

The experimental set-up is a reaction portal frame especially designed for beam elements under elevated temperatures. The specimens were heated by means of electroceramic resistances and a fibre mat specimen cover is used to increase the thermal efficiency. The material and the beam initial state conditions were considered, the experimental procedure being based on constant mechanical action under increasing thermal load.

The experimental data was compared with numerical solutions, obtained from a geometric and material nonlinear analysis. A shell finite element modelling, with incremental and iterative procedures, was used in the numerical calculations. Good agreement was obtained between experimental and numerical data. However, both numerical and experimental results lead to higher critical temperatures when compared with the simplified calculation procedure presented in Eurocode for this case.

© 2005 Elsevier Ltd. All rights reserved.

* Corresponding author. Tel.: +351 273303157; fax: +351 273313051.
E-mail address: ppiloto@ipb.pt (P.A.G. Piloto).

Keywords: Steel beams; Fire resistance; Lateral buckling; Critical temperature; Experimental tests; Numerical analysis

1. Introduction

Steel structures are widely used for building construction due to their mechanical properties. Due to the elevated costs in steel fire protection, several research studies have been carried out to predict the structural behaviour of steel members at high temperatures. Bailey et al. [1] performed several numerical calculations on lateral torsional buckling of steel beams for different degrees of utilisation. These authors used a uniform temperature distribution over the length and cross section and found that Eurocode 3, Part 1.2 overestimates the critical temperature in fire resistance calculations. Yin and Wang [2], using ABAQUS, presented the results of a parametric numerical study used to investigate the design factors in the lateral torsional buckling resistance and suggested a slenderness modification for steel beams with non-uniform temperature distribution.

Full scale experimental measurements made to assess the parameters which influence the behaviour of beams at elevated temperatures are hardly feasible due to the high costs and size limitations of horizontal furnaces. Vila Real et al. [3] conducted a set of experimental and numerical tests, performed in the resistance domain, on European series IPE100 beams subjected to high temperatures. The results obtained with temperatures varying from room conditions up to 600 °C lead to a new design formula for lateral torsional buckling that was adopted in the current version of part 1.2 of Eurocode 3 [4]. More recently, Vila Real et al. [5] presented new formulae, based on numerical simulations, which reduce the overconservative approach of part 1.2 of Eurocode 3 to the case of non-uniform bending load conditions.

Mechanical properties of steel deteriorate during fire and for conventional steel the yield strength at 700 °C is less than 23% of the specified value at room temperature. To improve the fire resistance of metallic structures, new steel alloys are being developed, the first ones in Japan, and present twice the tensile strength at 600 °C of conventional steel [6]. Therefore, conventional steels normally require fire protection to be applied. Thus, one important parameter to be determined is the critical temperature of each beam. This temperature is defined for the collapse condition and is a function of the degree of utilisation. In the present work, this parameter is assessed for a set of unrestrained beam elements, with a constant mid-span concentrated load, while temperature is constantly increased up to collapse; see Fig. 1.

2. Design limit state for laterally unrestrained beams

Steel I beams subjected to flexural loads have greater stiffness in the web plane than in the lateral plane. Unless these structural elements are properly braced they may collapse by lateral torsional buckling before their full in-plane capacity is attained. Lateral torsional buckling is a structural limit state where large displacements are combined with axial rotation.

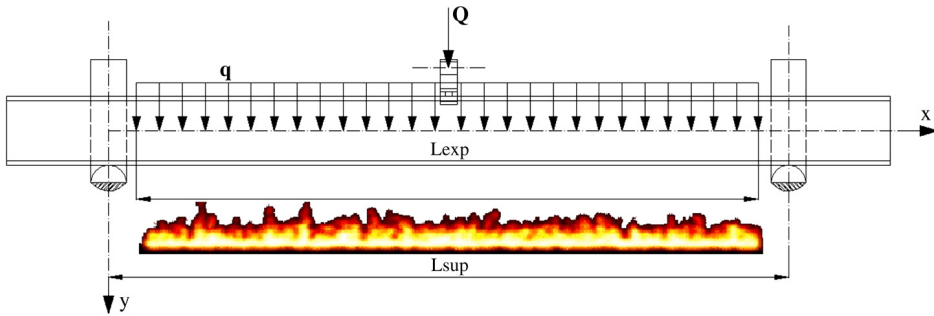


Fig. 1. Physical model under testing.

In Fig. 1 we schematically present the physical model used to produce a combined parabolic and triangular moment distribution, the latter being the most effective. The distributed load accounts for the self-weight of the beam and all the necessary equipment used for the heating process. The full scale tests were prepared to simulate in these loading conditions a degree of utilisation between 53% and 64% [4], as represented in Table 1.

As was explained previously, Eurocode 3, part 1.2 [4] presents overconservative results regarding the determination of the design buckling resistance, referred to as $M_{b,fi,t,Rd}$. The influence of the bending moment distribution on the lateral torsional buckling resistance appears, indirectly, through the value of the critical elastic moment. This parameter is obtained from the energy equation, as can be seen in Eq. (1):

$$\frac{M_Q}{M_{cr,M}} + \frac{M_q}{M_{cr,M}} = 1.423 \left[\sqrt{1 + \left(0.577 \frac{P_y y_Q}{M_{cr}}\right)^2} - 1.003 \frac{P_y y_Q}{M_{cr,M}^2} M_q + 0.577 \frac{P_y y_Q}{M_{cr,M}} - 0.167 \frac{M_q}{M_{cr,M}} \right] \quad (1)$$

where M_Q and M_q represent, respectively, the maximum bending moments due to the concentrated and distributed load, $M_{cr,M}$ equals the value of the uniform elastic critical moment, $P_y = \pi^2 E I_y / L^2$ and y_Q is the vertical position of the concentrated load.

According to the new proposal of Vila Real et al. [5], the design buckling resistance should account for a modified reduction factor $\chi_{LT,fi,mod}$ that takes into consideration the moment distribution over the beam length. This feature is responsible for the last two columns of Table 1, and increases the beam critical temperature by 20 °C, approximately.

Except when considering deformation criteria or when stability phenomena have to be taken into account, for a given steel component the critical temperature $\theta_{a,cr}$ at time t for a uniform temperature distribution may be determined, for any degree of utilisation μ_0 at time $t = 0$, using Eq. (2) [4]:

$$\theta_{a,cr} = 39.19 \ln \left[\frac{1}{0.9674 \mu_0^{3.833}} - 1 \right] + 482. \quad (2)$$

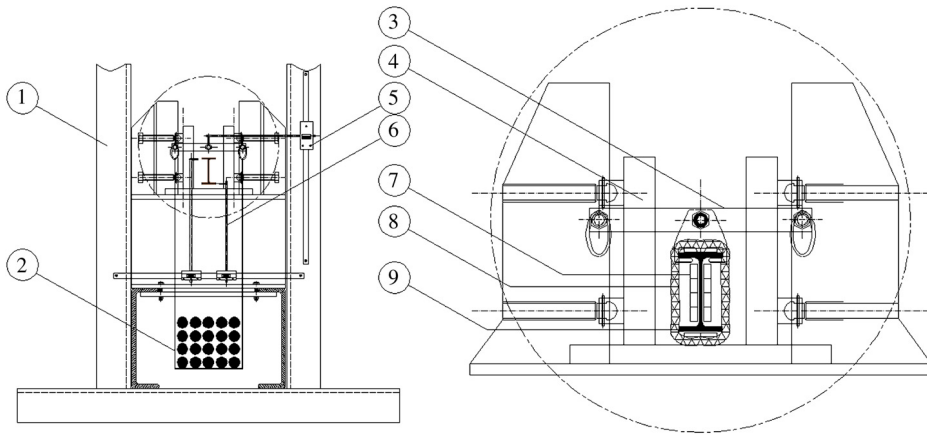


Fig. 2. Experimental set-up (load and displacement control).

Table 1

Applied load (degree of utilisation) and critical temperature design values

Beam effective length (m)	q (N/m)	Q (N)	$E_{fi,d} = \frac{QL}{4} + \frac{qL^2}{8}$	EC3-1.2 [4]		Vila Real et al. [5]		
				$\bar{\lambda}_{LT,\theta,com}$	$\mu_0 = \frac{E_{fi,d}}{R_{fi,d,0}} \theta_{a,cr}$ (°C)	$\mu_0 = \frac{E_{fi,d}}{R_{fi,d,0}} \theta_{a,cr}$ (°C)	$\theta_{a,cr}$ (°C)	
					[%]		[%]	
1.5	134.38	6086.12	2320.09	1.28	56	565.15	50	583.56
2.0	123.00	4315.52	2219.26	1.44	63	546.31	56	565.01
2.5	116.18	3043.06	1992.68	1.56	64	543.64	57	562.36
3.5	118.14	1521.53	1512.24	1.78	59	556.85	53	575.37
4.5	111.64	772.54	1151.69	1.97	53	575.48	47	593.86

For the lateral torsional buckling collapse mode, the critical temperature calculation requires an iterative procedure. The first step considers $M_{b,fi,0,Rd}$ at 20 °C, with the material reduction factors equal to unity, and then the critical temperature is calculated according to Eq. (2). The degree of utilisation needs to be updated during the following steps until convergence is attained.

3. Experimental model

A set of fifteen experimental full scale tests has been carried out using beams of the European series IPE 100 [7]. Beams with lengths varying from 1.5 to 4.5 m were tested using three tests for each beam length. The beams were heated by means of electroceramic mat elements, connected to a power unit of 70 kW. The thermal efficiency of the set-up was improved by using a ceramic fibre mat to insulate the beam.

As shown in Fig. 1, fork supports have been used in the rig to simulate a simple supported beam. In this figure, q represents the beam self-weight and the additional

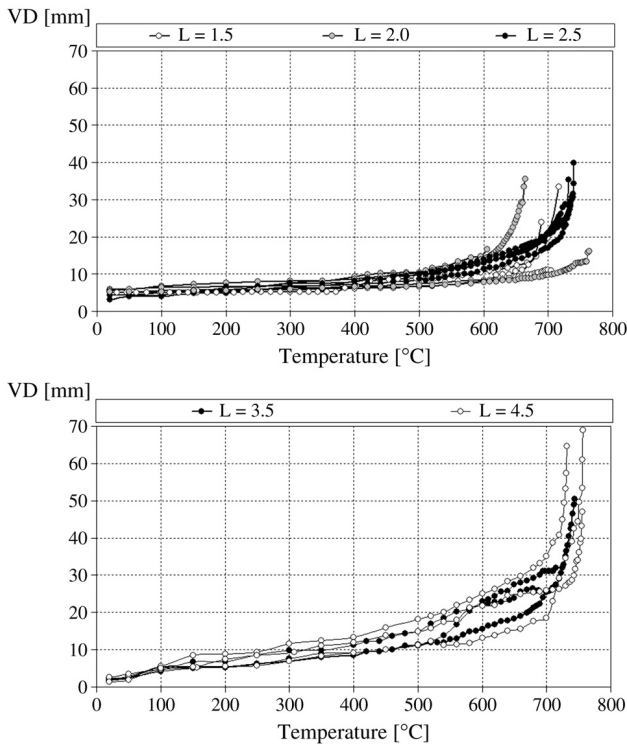


Fig. 3. Variation of vertical displacement with temperature.

distributed load due to the insulation mat and electroceramic resistances, Q being the applied dead load. To reduce the friction at supports, the distance $L_{\text{sup}} - L_{\text{exp}}$ equal to 0.2 m was left without protection.

The experimental set-up is represented in Fig. 2. The reaction frame (1), with two fork supports (4) was used to fix and load the beams (9). A balance system, represented by (3), was used to apply a dead load at a distance $y_Q = -0.105$ m from the shear centre. The loading support (2) was designed to maintain the vertical position throughout. Each beam was heated by means of an electroceramic resistance (7), protected by an insulation mat (8). Displacements were followed by three digital measuring rules (5, 6) used for lateral and vertical mid-span measurements.

3.1. Experimental procedure

Every tested beam was dimensionally controlled with the laser beam method to measure the initial out-of-straightness [7]. The measured values presented a maximum amplitude equal to $L/4000$, which is considered a small value when compared to the reference value $L/1000$. This last value was used in the numerical simulations.

To obtain the steel mechanical properties a set of 11 tensile specimens were extracted from the web of the beams and tested according to national standard NP EN 10002-1 [8].

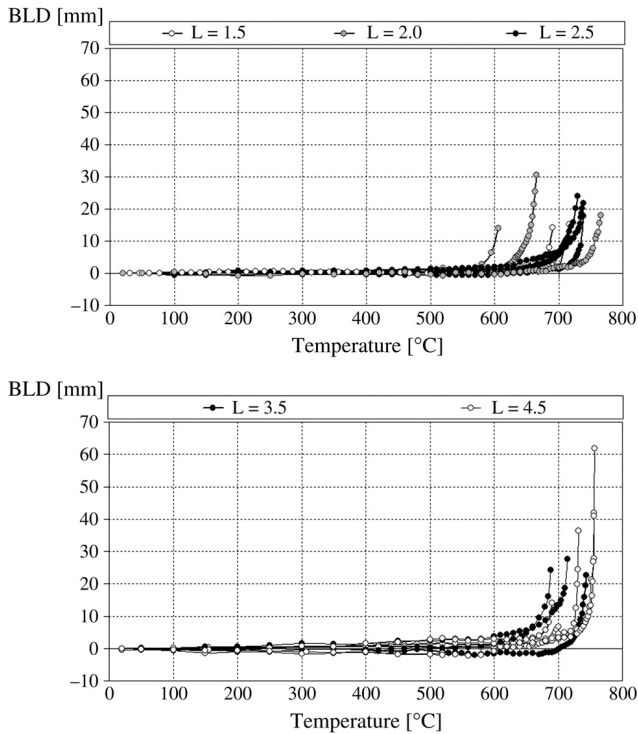


Fig. 4. Variation of bottom lateral displacement with temperature.

The yield strength $f_y = R_{eH} = 293.2$ MPa and the elastic modulus $E = 210$ GPa have been determined from the data average values and compared with the inspection certificate for the profiles.

The beams were loaded for a specific degree of utilisation, μ_0 , approaching real fire conditions. The mechanical load was specified according to typical values used. The degree of utilisation is the ratio between the design load effect and the beam resistance in fire conditions for time equal to zero, as represented according to Eq. (3). This coefficient is a function of the load type which, in this case, is predominantly a triangular moment distribution:

$$\mu_0 = \frac{E_{fi,d}}{R_{fi,d,0}} = \frac{M_Q + M_q}{M_{b,fi,0,Rd}} \quad (3)$$

The beam resistance should be calculated for the expected collapse mode (lateral torsional buckling). Table 1 presents the mechanical load applied on each beam, the slenderness values and the resultant critical temperature calculated by an iterative procedure.

In each test, after the beam had been loaded the temperature was increased at a constant rate of 800 °C/h controlled by a set of thermocouples, type k , placed along the beam length.

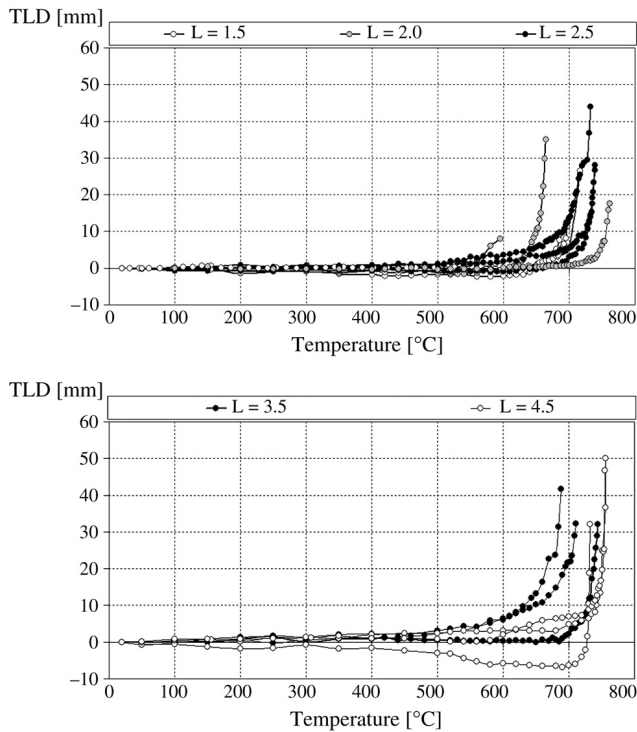


Fig. 5. Variation of top lateral displacement with temperature.

These thermocouples are used to provide the same heating rate for all electroceramic resistances, assuring a uniform temperature distribution on the exposed beam length; see Fig. 1.

For each beam, the vertical (VD) and lateral displacement (top (TLD) and bottom flange (BLD)) have been measured. The experimental data was used to obtain the temperature–displacement curves, represented in Figs. 3–5, for all tested beams.

All the tests were performed until a run-away deflection was achieved, the maximum mid-span displacement being shown in Table 2. Typical values used to determine the final stage of each test are based on the displacement or displacement rate for the vertical mid-span displacement. Those reference values are $L/20$ or a displacement rate of $L^2/9000d$, for vertical displacements higher than $L/30$, d being the distance from the top of the structural section to the bottom of the design tension zone [1]. Due to the width of the portal reaction frame used, the maximum vertical displacement measured is less than the reference values. Nevertheless, Figs. 6 and 7 show the on-going test and the ultimate state of one of the beams.

The critical temperature has been considered for the last measuring point, for which a small temperature increment produces a large lateral displacement. In Fig. 8, all measured critical temperatures have been registered, the experimental results being slightly greater than those obtained with the simple calculation formula [4]. This can be related to the

Table 2
Experimental critical temperature values

Buckling length (m)	Test run number	Critical temperature (°C)	Average critical temperature/SD (°C)	Maximum displacement (DV) ratio at mid-span
1.5	L1.5-1	717	704/13.5	L/45
	L1.5-2	690		L/63
	L1.5-3	705		L/137
2.0	L2.0-1	770	680/83.1	L/125
	L2.0-2	606		L/121
	L2.0-3	665		L/56
2.5	L2.5-1	732	737/4.6	L/71
	L2.5-2	740		L/73
	L2.5-3	740		L/63
3.5	L3.5-1	744	717/25.6	L/69
	L3.5-2	693		L/135
	L3.5-3	715		L/109
4.5	L4.5-1	732	748/14.2	L/70
	L4.5-2	757		L/65
	L4.5-3	756		L/96

small thermal insulation near supports, caused by the difference between L_{sup} and L_{exp} , introducing additional stiffness. Another possible cause may be related to the development of friction forces at the supports, producing extra axial restraints that, via the development of catenary action, reduce the beam deflection. This effect may delay the collapse, as was demonstrated by Yin and Wang [9].

4. Numerical model

The numerical analysis was based on a geometric and material non-linear programme, ANSYS [10]. Steel beams have been modelled by suitable shell finite elements normally used to model flat or warped, thin to moderately thick shell structures. This element (shell 181) has six degrees of freedom at each node, translations in the nodal x , y and z directions and rotations about the same axes. The deformation shape functions are linear in both in-plane directions and present two integration points for in-plane and five for normal directions. A high rigid beam finite element was used to simulate exactly the application point of the load.

The beam cross section was modelled with mid-plane dimensions and the stress/strain relations are based on the Eurocode 3 elastic–elliptic–plastic model; see Fig. 9. The yield stress at room temperature was obtained from the tensile tests performed. In the calculations the elastic modulus and the thermal elongation vary with temperature also, in agreement with Eurocode 3, the other mechanical properties being considered constants.



Fig. 6. Experimental on-going test run.

Every structural element presents initial imperfections due to fabrication processes, transportation, storage and construction methods. The initial out-of-straightness imperfection causes a secondary bending moment as soon as any compression load is applied, which in turn leads to further bending deflection and a growth in the amplitude of this bending moment lever arm. Stable deflected shape equilibrium can be established until the internal compression force does not exceeds the internal moment resistance. The numerical model was implemented with an initial out-of-straightness represented by a harmonic function with $L/1000$ as the maximum amplitude.

Residual stresses were also considered, on the basis of a theoretical distribution (bi-triangular shape), with a maximum value of 30% of the material yield stress. Numerically, these initial residual stresses were introduced at the element integration points, as represented in Fig. 10. However, as explained in [11], the beam buckling resistance is less sensitive to the residual stresses when subjected to high temperatures.

The numerical model has been implemented with four finite shell elements in the web and the same number over the beam flanges. The beam ends were modelled by two fork supports, constraining vertical and lateral displacements and letting the beam warp freely. An iterative procedure was implemented using material and geometric non-linear behaviour and temperature increments at a specific rate of $800\text{ }^{\circ}\text{C/h}$. To simulate the beam heating an autosteppping method, based on the temperature field imposed over each node,

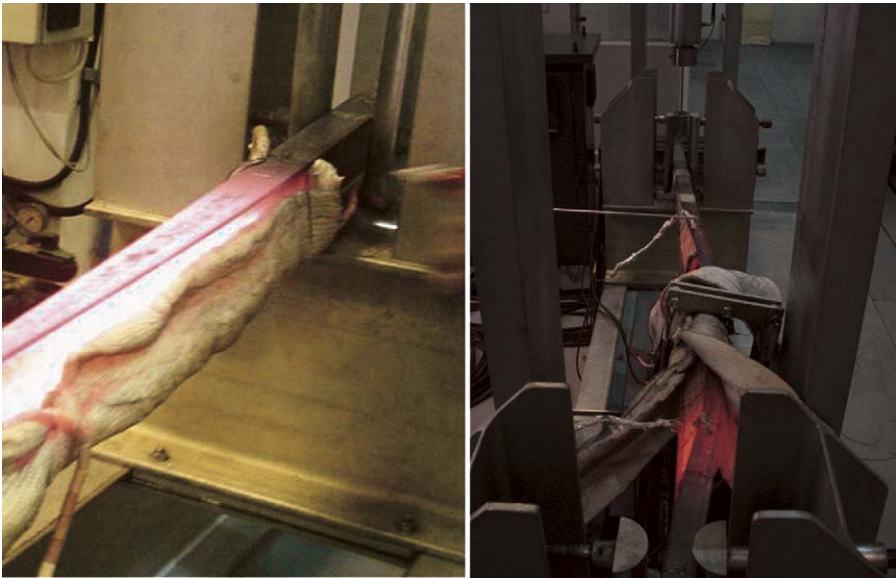


Fig. 7. Final stage of experimental test run.

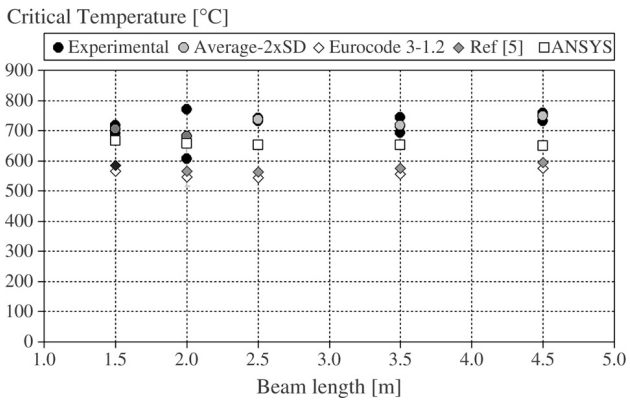


Fig. 8. Critical temperature results for all beams tested.

was used. In the numerical simulation a uniform temperature distribution over the whole beam was considered.

The critical temperature was defined as the last temperature at which the equilibrium was maintained. The numerical results determined for the critical temperature, represented in Fig. 8, are compared with the simplified design formula and with experimental data. The numerical results are always greater than the values from the simplified prediction.

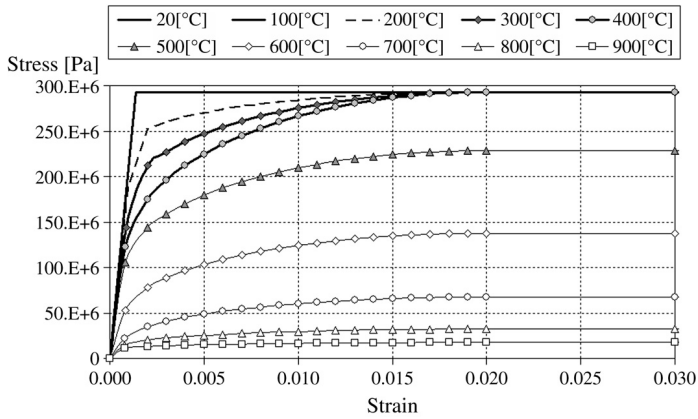


Fig. 9. Conventional steel stress–strain curve at elevated temperatures.

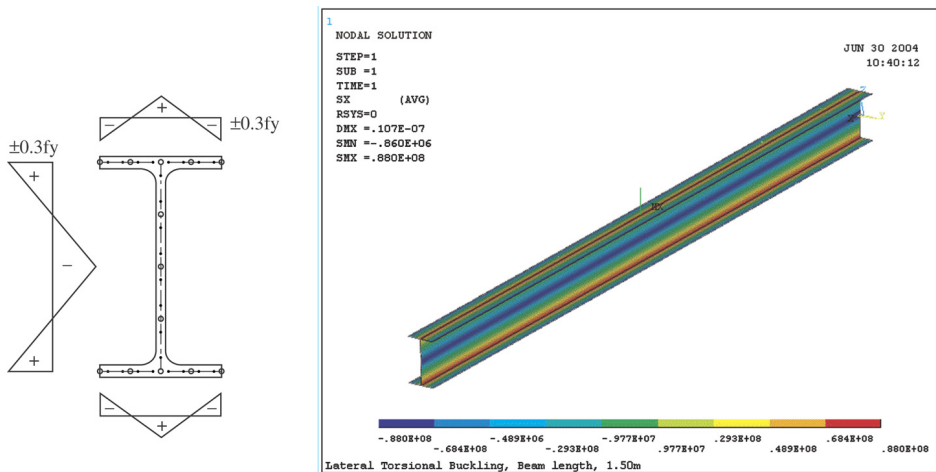


Fig. 10. Residual stress model applied to shell elements.

5. Conclusions

The critical temperature has been determined for several laterally unrestrained beams, on the basis of a numerical and experimental procedure. The beams tested were subjected to a constant load and then an increasing temperature was applied, approaching fire accident conditions.

A small dispersion was obtained in the experimental data resulting from each set of experiments. Both numerical and experimental results lead to higher critical temperatures in comparison with the simplified design calculation procedure for this instability phenomenon. Thus, Eurocode formulae may lead to conservative results, as was already demonstrated in Ref. [5].

Higher critical temperatures obtained in the experimental tests are possibly related to the non-uniform temperature distribution near the supports. This effect leads to a small increase in the beam stiffness. Another effect with an influence on the results that should be investigated is related to the shape of the fork supports. These elements may introduce a restriction on lateral rotation and some friction in the longitudinal displacement of the beam. The results obtained correlate well with previous work by the research team and prove that a conservative design is obtained when Eurocode 3 is used.

Acknowledgments

This work was performed during the European research project INTERREG III-A, RTCT-B-Z/SP2.P18, whose support is gratefully acknowledged. Special thanks are also due to the J. Soares Correia Company for the kind provision of the steel beams.

References

- [1] Bailey CG, Burgess IW, Plank RJ. The lateral–torsional buckling of unrestrained steel beams in fire. *J Constr Steel Res* 1996;36(2):101–19.
- [2] Yin YZ, Wang YC. Numerical simulations of the effects of non-uniform temperature distributions on lateral torsional buckling resistance of steel I-beams. *J Constr Steel Res* 2003;59:1009–33.
- [3] Vila Real PMM, Piloto PAG, Franssen J-M. A new proposal of a simple model for lateral–torsional buckling of unrestrained steel I-beams in case of fire: experimental and numerical validation. *J Constr Steel Res* 2002; 59(2):179–99 [Elsevier Science].
- [4] CEN prEN 1993-1-2. Eurocode 3, design of steel structures—part 1–2: General rules—structural fire design. April 2003, stage 49 draft.
- [5] Vila Real PMM, Lopes N, Silva LS, Franssen J-M. Lateral torsional buckling of unrestrained steel beams under fire conditions: improvement of EC3 proposal. *Comput Struct* 2004;82:1737, 1744.
- [6] Ding J, Li G-Q, Sakumoto Y. Parametric studies on fire resistance of fire resistant steel members. *J Constr Steel Res* 2004;60:1007–27.
- [7] Mesquita LMR. Thermo-mechanical instability of beams subjected to elevated temperatures. Numerical and experimental study. Master of science thesis, July 2004 [in Portuguese].
- [8] NP EN 10 002-1. CT12, Metallic materials: Tensile Tests. Part 1: Test methodology. Portuguese Institute for Quality; 1990 [in Portuguese].
- [9] Yin YZ, Wang YC. A numerical study of large deflection behaviour of restrained steel beams at elevated temperatures. *J Constr Steel Res* 2004;60:1029–47.
- [10] Ansys INC. ANSYS user's manual. 2003.
- [11] Vila Real PM, Cazeli R, Simões da Silva L, Santiago A, Piloto P. The effect of residual stresses in lateral torsional buckling of steel I-beams at elevated temperature. *J Constr Steel Res* 2003;60(3–5):783–93.